

Learning Hand-Held Object Reconstruction from In-The-Wild Videos

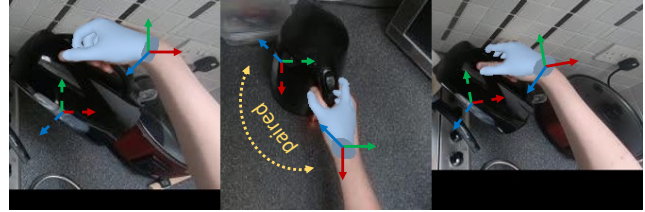
Aditya Prakash Matthew Chang Matthew Jin Saurabh Gupta
 University of Illinois Urbana-Champaign
<https://ap229997.github.io/projects/horse>



1(a) Task. We tackle 3D reconstruction of hand-held objects from single in-the-wild images, e.g. the dart in this YouTube video frame.



1(b) Key Idea. We use multiview supervision from large scale in-the-wild video datasets. This clip of a person using a kettle provides multiple views of the kettle (thus revealing its 3D shape) without the person intending to do so. We refer to this as *incidental multiview supervision*. Leveraging this supervision from videos at scale can enable better generalization to novel in-the-wild objects at test time.



1(c) Unknown pose. Existing multiview reconstruction approaches do not work in our setting due to unknown camera poses & estimating them using COLMAP [59] is hard due to insufficient feature matches across views. Assuming hand & object move rigidly lets us use hand pose, estimated by FrankMocap [56], as a proxy for object pose, thereby giving us camera pose in all views. This helps us exploit the scale of in-the-wild videos for multiview training.



1(d) Handling occlusions. Objects are often occluded by hands and other entities (left). To mitigate this issue, we learn shape priors for hand-held objects using synthetic object datasets (right).

Abstract

Prior works for reconstructing hand-held objects from a single image rely on direct 3D shape supervision which is challenging to gather in real world at scale. Consequently, these approaches do not generalize well when presented with novel objects in in-the-wild settings. While 3D supervision is a major bottleneck, there is an abundance of in-the-wild raw video data showing hand-object interactions. In this paper, we automatically extract 3D supervision (via multiview 2D supervision) from such raw video data to scale up the learning of models for hand-held object reconstruction. This requires tackling two key challenges: unknown camera pose and occlusion. For the former, we use hand pose (predicted from existing techniques, e.g. FrankMocap) as a proxy for object pose. For the latter, we learn data-driven 3D shape priors using synthetic objects from the ObMan dataset. We use these indirect 3D cues to train occupancy networks that predict the 3D shape of objects from a single RGB image.

Our experiments on the MOW and HO3D datasets show the effectiveness of these supervisory signals at predicting the 3D shape for real-world hand-held objects without any direct real-world 3D supervision.

1. Introduction

Understanding how humans use their hands to interact with real-world objects in daily tasks is crucial for applications in AR/VR [5, 21] and robotics [37, 38, 49, 50, 71, 73]. Yet, building such an understanding is difficult since hands interact with objects in diverse ways and objects are often occluded. As a step towards an improved understanding of hand-object interactions, we study the problem of 3D reconstruction of hand-held objects from a single image in the wild (Fig. 1a).

Collecting datasets with ground truth 3D shapes for hand-held objects is hard. Existing hand-object datasets are typically collected in lab settings using visual scanning setups

(via multiple RGB/ RGB-D cameras or motion capture) limiting their diversity. Synthesising realistic hand-object interaction is an open problem in itself [29, 32, 51, 69] which precludes the use of purely synthetic training. Another option is manual alignment of template shapes [7], which is both approximate and difficult to scale. Thus, there is very little in-the-wild real-world data with ground truth 3D shapes for hand-held objects. Several works [24, 32, 74] have designed expressive models to predict shapes of hand-held objects but they are all held back by limited 3D supervision available for training. This limits the generalization capability of existing approaches to novel objects encountered in the wild.

While direct 3D supervision is limited, there is an abundance of in-the-wild videos showing hand-object interactions [9, 19, 62]. Can we somehow learn about the 3D shapes of hand-held objects from these videos to scale up learning, thus improving generalization to novel objects? We observe that these videos *incidentally* show different views of the same hand-held object (Fig. 1b) and thus provide cues for learning about their shape [22]. This is different than lab setting where people often rotate objects intentionally to capture different views. In this paper, we design methods to extract this *incidental multiview supervision* to scale-up learning of models to predict 3D shapes for hand-held objects.

A key challenge in incidental multiview supervision is unknown camera pose, which precludes the use of existing multiview reconstruction approaches [45, 59, 60, 72]. While there exist structure from motion (SfM) techniques, *e.g.* COLMAP [59, 60], to estimate camera pose, they do not work in our setting due to lack of sufficient feature matches across different views. We sidestep this problem by using hand pose as a proxy for object pose (Fig. 1c). This is based on the observation that in many situations the hand and the object move together rigidly (humans rarely conduct in-hand manipulation in pick & place tasks involving rigid objects). In such a situation, the relative pose of the hand between pairs of frames reveals the relative pose of the object. This reduces the SfM problem to an easier setting where the motion is known. Specifically, we use advances in hand pose estimation, FrankMocap [56], to obtain pose for the hand and consequently the object pose in all views. We then use the estimated poses along with object segmentation masks, either available or predicted using existing hand-object segmentation model [11] to generate supervision for 3D object reconstruction.

While this works well for unoccluded parts of the object, this does not generate reliable supervision for parts of the object that are occluded by the hand (Fig. 1d). To address this limitation, we build priors for shapes of hand-held objects and supervise the model to predict shapes that look like hand-held objects. The model can thus learn to output contiguous shapes even when the object is interrupted by the hand in the image, *e.g.* it can hallucinate a handle for a jug

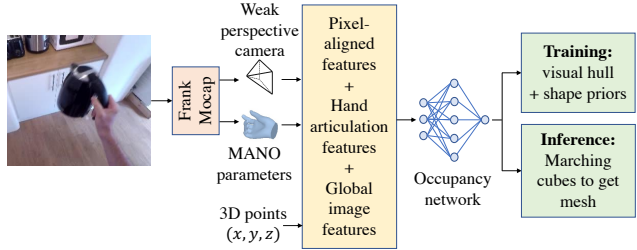


Figure 2: Pipeline. The input image is passed through FrankMocap [56] to get the MANO hand parameters and weak perspective camera. Following Ye *et al.* [74], we sample the 3D points in hand coordinate frame and compute pixel-aligned features by projecting points into the image and hand articulation features by transforming points into coordinate frame of each hand joint. We pass these features into an occupancy network to predict the 3D occupancy for each of the sampled points. **Our contribution** is in training this model using multiview 2D mask supervision (Sec. 3.2, Fig. 3) and shape priors (Sec. 3.3, Fig. 4). At inference, we predict occupancy for $64 \times 64 \times 64$ uniformly sampled points in a $[-1, 1]^3$ volume, and run marching cubes to get the object mesh. Note that 2D object masks are only used during training and not at test time.

even when it is covered by the hand, because jugs typically have one. We adopt an adversarial training framework [18] to train a discriminator to differentiate between real shapes (sampled from ObMan dataset) and shapes predicted from the model, thus serving as a prior. The model is supervised to predict shapes that look real under the learned discriminator.

At test time, we only have access to single images, therefore we incorporate these indirect supervision cues in the latest work on hand-held 3D reconstruction from single image from Ye *et al.* [74]. and train on video sequences curated from the VISOR dataset. Their formulation predicts the object shape, represented as signed distance fields [46], from an input RGB image in the MANO hand coordinate frame [54] obtained from FrankMocap [56]. We modify their formulation to represent shapes via occupancy [42] since it worked better in our setting. Our full pipeline is shown in Fig. 2. We believe our work opens the door to learning models for reconstructing hand-held objects using in-the-wild data.

Contributions: (1) We exploit in-the-wild videos showing hand-object interactions for 3D reconstruction of hand-held objects from a single image. (2) We use incidental multiview 2D supervision and data-driven 3D shape priors to train occupancy networks to predict 3D shape, thereby circumventing the need for real-world 3D supervision. (3) We demonstrate the effectiveness of these supervision cues for predicting shapes for novel objects on the challenging MOW dataset and achieve state-of-the-art performance.

2. Related Work

Multiview 3D reconstruction. Predicting 3D shape from multiple views has been extensively studied. Given a collection of images of the same scene, earlier works focus

on SfM approaches [1, 14, 22, 27, 58–61, 65, 78] to estimate the camera parameters and sparse 3D structure of the scene. These sparse reconstructions are then passed through multi-view stereo techniques [4, 15, 16, 16, 17, 63, 64, 77] to recover dense 3D structure. The recovered 3D shape can be represented in several ways: voxels [40], point cloud [47, 48] meshes [67], SDFs [46], occupancy [42], radiance fields [43], canonical surface maps [33]. More recently, implicit shape representations [42, 46] have gained traction since they can represent shapes compactly at arbitrary resolution using a neural network, which can then be queried to predict the SDF or occupancy at different points in space. Following recent trends, we also use implicit representation in our work.

3D Shape from a single image. Past works have studied single image shape cues, *e.g.* shape from texture [2, 6], shading [76], silhouette [13] for predicting 3D shape from a single image. As the problem is under-constrained, researchers have focussed on building good priors for shapes and associated factors: albedo and illumination [12]. Recent works have cast this as a learning problem [42, 46] which automatically extracts the relevant priors from training datasets that contain images paired with 3D shape supervision. Training can be done on synthetic datasets [8] or on real-world datasets collected using SfM techniques [59, 60] or depth sensors [16]. Our work also falls in this paradigm since we focus on 3D reconstruction of hand-held objects from a single image, but we do not use real-world 3D supervision.

3D from single image without direct 3D supervision. Several works have sought to relax the need for direct 3D supervision for training shape prediction models. The key idea is to convert multi-view shape cues into loss functions for training. Early papers [79] learned to predict depth from a single image by enforcing photometric consistency when projecting to another view according to the predicted depth. This idea has been extended to leverage consistency in masks, depth, or RGB to predict complete 3D shapes from single images [68]. Recent works also incorporate different priors for constrained shape prediction. *E.g.* Kanazawa *et al.* [30] leverage 2D keypoint re-projection along with a learned prior on relative 3D joint angles for estimating 3D shape and pose for people. Similar approaches have been applied to reconstruction of category-specific [31] as well as generic objects [75]. In this work, we use multiview supervision from 2D object masks to circumvent the need for 3D supervision.

Reconstructing Hand-held Objects. Advances in single image 3D shape prediction have been applied to predicting shape for hand-held objects [74], and for joint reasoning about hand and object shape [24, 32]. Recent works [7, 23] adopt a test-time optimization approach to align 3D shape templates to images [7] and videos [23]. However, Ye *et al.* [74], Hasson *et al.* [24], and Karunratanakul *et al.* [32] all rely on 3D supervision and train in simulation or on small-scale real-world datasets. Instead, we circumvent the

need for real-world 3D supervision by using multiview 2D supervision from in-the-wild videos. Concurrent work from Huang *et al.* [28] fits a radiance field [43] to reconstruct hand-held objects from videos captured in lab settings. In contrast, we use in-the-wild videos at training time only, and can make predictions from a single image at test time. [36, 70] also use the hand and human body to establish correspondences between views for reconstruction at test time.

Understanding Hands and Objects of Interaction. There is a growing interest in understanding hands and how they interact with objects around them. Researchers have collected datasets and trained models for detecting and segmenting hands and associated objects of interaction [11, 62]. Recognizing what hands are doing in images has also been well studied: through grasp classification [32], 2D pose estimation [53, 80], and most recently 3D shape and pose estimation [24, 55, 56]. Specifically, we build upon the FrankMocap detector from Rong *et al.* [56], that outputs MANO hand parameters [55] from input RGB images, and the hand conditioned object reconstruction framework of Ye *et al.* [74].

3. Approach

We propose a method for training shape predictors for hand-held objects that does not require ground truth 3D shape information for training. As our focus is on the supervision signals, we adopt and modify the recent state-of-the-art AC-SDF architecture for this task from Ye *et al.* [74]. Given an input RGB image, AC-SDF uses an implicit SDF representation [46], for the object, in the hand coordinate frame and trains the model using direct 3D supervision on the SDF values. We instead derive training supervision by considering consistency between the projection of object in different views, and priors on shapes of hand-held objects. While we build on top of the recent AC-SDF model from Ye *et al.* [74], our loss functions are general and can be used with any methods that predict SDFs or occupancies.

3.1. Preliminaries

Given an input RGB image, AC-SDF uses a neural network to predict the SDF of the object. AC-SDF’s key innovation is in conditioning the SDF prediction on the articulation state of the hand. Thus they operate in the hand coordinate frame obtained using FrankMocap [56], which outputs a) hand articulation parameters θ^a (45 dimensional MANO hand pose parameters [54]), b) the 6 DOF global rotation and translation θ^w of the wrist joint, and c) a weak perspective camera that is converted to a full perspective camera K . θ^a provides information about the articulation state of the hand, θ^w is used to transform predictions in the wrist coordinate frame back into the camera coordinate frame for final prediction, and K & θ^w together enable the projection of a point in the wrist coordinate frame onto the image plane via $\mathbf{x}_p = \pi_{\theta^w}(\mathbf{x}) = K^T \theta^w \mathbf{x}$.

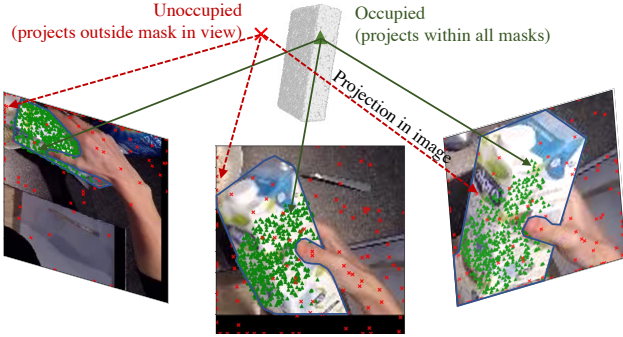


Figure 3: Supervision from masks in multiple views. We use 2D segmentation supervision in multiple views for labeling 3D points with occupancy. 3D points that project into the object mask in all views are considered as occupied (green triangles), all other points are considered unoccupied (red crosses). It is also possible that certain object points may not project into the mask in the image due to incorrect hand poses. Note that the 3D object in the figure is for visualization only (not used for sampling).

Given a 3D point \mathbf{x} , AC-SDF predicts the SDF value for \mathbf{x} using: a) global image features from a ResNet-50 [26], b) pixel-aligned features [57] from intermediate layers of ResNet-50 encoder at the location \mathbf{x}_p where \mathbf{x} projects into the image, and c) hand articulation features obtained by representing \mathbf{x} in the coordinate frame of the 15 hand joints. Predicted SDF values are supervised using ground truth SDF value from annotated 3D shapes on synthetic (ObMan [24]) and real datasets (HO3D [20] or MOW [7]).

We adopt the AC-SDF architecture with one modification: we predict occupancy instead of SDFs. We find training with occupancy prediction to be more stable than predicting SDFs. We denote the full function realized by AC-SDF as $\mathbf{s} = f(\mathbf{x}; I, \theta^a, \theta^w, K)$. Given the input image I , hand articulation parameters θ^a , 6DOF wrist pose θ^w and camera parameters K , it predicts the occupancy \mathbf{s} at 3D location \mathbf{x} .

3.2. Supervision from Masks in Multiple Views

We supervise the function f via consistency in masks in multiple views of the object. Let’s assume we have multiple views $\{I_1, \dots, I_n\}$ showing the same hand-held object. We further assume that the hand is rigidly moving with the object. This is not an unreasonable assumption, as humans rarely do in-hand manipulation in pick & place tasks involving small rigid objects. We also assume segmentation masks for objects of interaction in these n views and denote them as $\{M_1, \dots, M_n\}$. These can be obtained using recent state-of-the-art models [25] for segmenting objects of interaction [11]. We also obtain predictions for hand articulation, 6 DoF wrist pose, and camera intrinsics for each of these n frames using FrankMocap (as described in Sec. 3.1): $\{(\theta_1^a, \theta_1^w, K_1), \dots, (\theta_n^a, \theta_n^w, K_n)\}$.

Given this multi-view setup, our supervision for $f(\mathbf{x}; I_1, \theta_1^a, \theta_1^w, K_1)$ comes through consistency with seg-

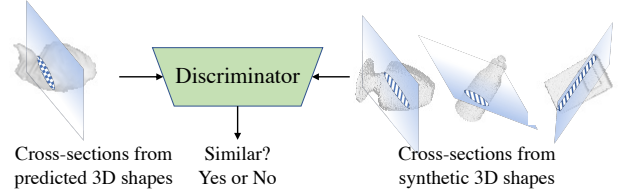


Figure 4: Shape priors. We learn data-driven 3D shape priors using hand-held objects from ObMan dataset. We sample planes through the object (shown above in blue), resulting in a 2D cross-section map. We pass occupancy on these cross-sections through a discriminator which tries to distinguish cross-sections of predicted 3D shapes from cross-sections of ObMan objects.

mentations in different views. Specifically, we project \mathbf{x} into the different views using θ_i^w to obtain $\mathbf{x}_{p_i} = \pi_{\theta_i^w}(\mathbf{x})$. Note that since \mathbf{x} is in the wrist coordinate frame, it can be projected into different views using the 6DOF wrist pose θ_i^w in I_i and the camera intrinsics K_i . We show examples of points which project into the object mask in different views in Fig. 3. With this projection, we get occupancy labels for a point \mathbf{x} as $\mathbf{s}^{gt} = \cap_{i=1}^n M_i(\mathbf{x}_{p_i})$ and train using $\mathcal{L}_{\text{visual-hull}} = \text{CE}(\mathbf{s}, \mathbf{s}^{gt})$ where CE is cross-entropy loss and $\mathbf{s} = f(\mathbf{x}; I, \theta^a, \theta^w, K)$ is the predicted occupancy at \mathbf{x} .

This is reminiscent of the visual hull algorithm [34, 41], which generates 3D reconstruction by carving out space that projects outside the segmentation in any view. Visual hull algorithms need multiple views at *test* time to generate any output. In contrast, we are doing this at training time to obtain supervision for $f(\mathbf{x}; I_1, \theta_1^a, \theta_1^w, K_1)$, which is a single image model and can be used at test time to obtain shape predictions from a single view.

To further regularize training, we employ another loss that encourages object shape prediction from different views to be consistent with each other. Since our predictions are already in the hand coordinate frame, which is common across all views, this can be done by minimizing $\mathcal{L}_{\text{consistency}} = \sum_{\mathbf{x} \in \mathbb{R}^3, i \neq j} \text{CE}(f(\mathbf{x}; I_i, \theta_i^a, \theta_i^w, K_i), f(\mathbf{x}; I_j, \theta_j^a, \theta_j^w, K_j))$ for all different views i and j of the same object.

3.3. Hand-held Object Shape Prior Supervision

Our next source of supervision comes from reasoning about shapes of hand-held objects. To this end, we a) build a prior on shapes of hand-held objects, and b) use the prior to supervise the training of the occupancy prediction function $f(\mathbf{x}; I, \theta^a, \theta^w, K)$. As such a prior can be challenging to hand-craft, we build it in a data-driven way using existing repositories of 3D shapes [8, 24]. Specifically, we adopt an adversarial training framework [18] and jointly build this prior while providing the supervision for training f . We train a discriminator g to differentiate between real (synthetic shapes from ObMan dataset) and generated shapes (shapes predicted by f). We derive supervision for f by encouraging it to predict shapes that are real as per the discriminator g .

Building this prior in 3D is computationally challeng-

ing. Instead, we build this prior on occupancy values in arbitrary 2D slices (that pass through the origin) of real and predicted 3D shapes. For generated samples, this involves sampling the function f on a 2D grid placed on a random plane passing through the origin. We adopt the same strategy for representing real samples, but use the predictions of the model on the ObMan training set. As these are predictions on the ObMan training set, they generally match the ground truth slices well but at the same time are soft and prevent the discriminator from cheating.

Supervision for f is obtained by computing gradients through g on the sampled occupancy values so as to maximize the realism of the occupancy slices output by f . Following [30], we use the least squares formulation [39] for training the discriminator. The shape prior loss takes the form $\mathcal{L}_{\text{shape-prior}} = g(\text{slice}(f(\cdot; I, \theta^a, \theta^w, K)))^2$, where slice function samples a 2D slice using the occupancy function f , and g is the discriminator that has been trained to predict 0 for real samples and 1 for generated samples using L2 loss.

4. Processing in-the-wild VISOR videos

VISOR [11] is a recent dataset that provides labels for short video snippets from the EPIC-KITCHENS dataset [10] with tracks for hands & objects they are interacting with and their segmentation masks. It provides a rich set of hand-object interactions, *e.g.* taking out milk from fridge, pouring oil from bottle, kneading dough, cutting vegetables, and stirring noodles in a wok. Our interest is in the reconstruction of *rigid* objects which are *in-contact* with a hand. Hence, we employ a combination of automated and manual filtering, both at the level of snippets and the frames within a snippet, to prepare a dataset for training our model.

We start with some automated filtering based on contact annotations that come with the dataset. We select object tracks where one and only one hand is in consistent contact with the object. This removes tracks that are entirely on background objects or have multiple hands involved (*e.g.* kneading dough). If the object within a sequence interacted with both left and right hands in separate frames (*e.g.* object is moved from one hand to the other), the sequence is split into two subsequences, one for each hand. This leaves us with 14768 object tracks from the original VISOR dataset.

Next, we manually filter the dataset to select a subset that showcases manipulation of rigid objects with a single hand. We also remove data with significant motion blur, occlusion, and image border clipping. This leaves us with 604 video snippets showing 144 different object classes being interacted with. These 604 snippets have 3.25 frames on average and span an average duration of 0.5 seconds.

Automatic removal of frames with incorrect hand predictions. While this subset of data is fit for training, we rely on the 3D hand pose predicted by FrankMocap to set up the output coordinate frame, compute hand articulation fea-



Figure 5: VISOR visualizations. Using existing hand pose estimation techniques [56], we are able to track the objects in relation to hands through time in in-the-wild videos. We visualize these tracks along with object masks from the VISOR dataset [11]. This form of data, where objects move rigidly relative to hands, is used to train our proposed formulation to learn 3D geometry of hand-held objects from in-the-wild videos.

tures, and more importantly to register the different frames together. Thus, we require decent 3D hand pose predictions. We employ automated filtering using the uncertainty estimate technique from Bahat & Shakhnarovich [3] that has been shown to be effective for estimating uncertainty in 3D human pose prediction [52]. Specifically, we obtain 3D hand pose predictions on five different versions of the image, augmented by different fixed translations. The uncertainty estimate for a given image is computed as the standard deviation of reprojection locations of MANO vertices across these 5 image versions. This sidesteps the need to hand-specify the trade-off between translation, rotation, and articulation parameters that are part of the 3D hand pose output. This leaves us with 473 video snippets consisting of different objects. We show some example object sequences in Fig. 5. Note the *incidental* multiple views and relative consistency in hand and object pose over the course of interaction.

5. Experiments

Datasets. We use a combination of datasets for training and testing. For testing we use the HO3D [24] and MOW [7] datasets. Both these datasets contain real images with 3D ground truth. HO3D shows the 10 YCB objects [81] from multiple views in lab settings, while MOW consists of 391 images spanning 120 object templates sampled from YouTube videos. As our method does not require 3D ground truth, we do not use these datasets for training our models, but only for evaluations. Many baselines we consider require 3D ground truth for training. We train them on HO3D when testing on MOW and train on MOW when testing on HO3D. For HO3D, we adopt the splits used by [74] and use the 1221 testing images across the 10 objects. Almost all of our ex-

Method	Dataset and supervision used	F@5 \uparrow	F@10 \uparrow	CD \downarrow
<i>Object generalization experiment on in-the-wild MOW [7]</i>				
AC-OCC	ObMan (Synthetic 3D)	0.095	0.179	8.69
AC-SDF [74]	ObMan (Synthetic 3D)	0.108	0.199	7.82
AC-SDF [74]	ObMan (Synthetic 3D) + HO3D (Lab 3D)	0.082	0.159	7.52
Ours (HORSE)	ObMan (Synthetic 3D) + VISOR (Multi-view 2D)	0.121	0.220	6.76
<i>Object generalization experiment in lab setting on HO3D [24]</i>				
AC-OCC	ObMan (Synthetic 3D)	0.181	0.331	4.39
AC-SDF [74]	ObMan (Synthetic 3D)	0.175	0.329	3.72
AC-SDF [74]	ObMan (Synthetic 3D) + MOW (Real 3D)	0.174	0.334	3.63
Ours (HORSE)	ObMan (Synthetic 3D) + VISOR (Multi-view 2D)	0.198	0.352	3.39

Table 1: Object generalization results. We report F-score at 5mm & 10 mm, Chamfer distance (CD, mm) for object generalization splits on MOW and HO3D. We compare with AC-OCC & AC-SDF baselines trained on different combinations of datasets with full 3D supervision. Our approach outperforms baselines across all metrics without using real-world 3D supervision in both in-the-wild & lab settings.

periments are conducted in the *object generalization setting* where we assess predictions on novel objects across datasets. For completeness and further analysis, we also test in the *view generalization setting on HO3D* as used in [74] where predictions are made on novel views of training objects.

Following past work [24, 32, 74], we include synthetic data with 3D ground truth from the ObMan dataset [24] for training all models. The ObMan dataset consists of 150k images showing 2.5k different objects grasped in configurations computed using GraspIt [44]. Our method additionally uses videos of hand-held objects for training. We primarily use the VISOR dataset as a source of these in-the-wild hand object interaction videos. Note that none of these datasets have 3D ground truth associated with them and hence they can not be used to train the baseline models.

Metrics. To evaluate the object reconstruction quality, we first extract a mesh, using marching cubes, from the predicted occupancy or SDF on a set of points uniformly sampled in a $64 \times 64 \times 64$ volume. Following prior works [66, 74], we report Chamfer distance (CD) and F1-score at 5mm and 10mm thresholds. The F1-score evaluates the distance between object surfaces and is defined as the harmonic mean between precision and recall. Precision measures the accuracy of the reconstruction as the % of reconstructed points that lie within a certain distance to the ground truth. Recall measures the completeness of the reconstruction as the % of points, on the ground truth, that lie within a certain distance to the reconstruction. CD computes the sum of distances for each pair of nearest neighbors in the two point clouds. We report the mean CD & F-score over all objects in the test set.

Baselines. We compare our model with the AC-SDF model trained on ObMan +MOW & ObMan +HO3D datasets, in supervised manner using 3D ground truth, and then evaluate on HO3D and MOW object generalization splits respectively. We also compare with an occupancy variant of AC-SDF by

replacing the SDF formulation with an occupancy network (AC-OCC). Note that the VISOR dataset cannot be used for training since it does not have 3D supervision. For the view generalization setting on HO3D, we also consider compare against HO [24] and GF [32]. Existing structure from motion pipelines, *e.g.* COLMAP [59, 60], do not work in our setting due to a lack of feature matches between different views, since the objects are occluded. Recent works [45, 72] on unsupervised reconstruction of objects require several views or depth, which are not available in our setting.

Implementation Details. We adopt architecture of Ye *et al.* [74] (Sec. 3.1) and experiment with both DeepSDF [46] & Occupancy Networks [42]. We find the latter to work better in our setting. The architecture consists of an 8-layer MLP with 512 hidden units and a skip layer. We sample 8192 points in the hand coordinate frame for training the occupancy network, out of which 4096 points are sampled such that they project inside the object mask in every view. 778 points are sampled on the hand mesh and the rest of the points are sampled uniformly in a $[-1, 1]^3$ volume centered at the hand. The points projecting inside the object masks in all views are labeled as occupied and all the other points are labeled as unoccupied. We adopt mixed dataset training where our model is trained simultaneously using synthetic 3D supervision on ObMan and 2D supervision on VISOR. We set the dataset ratio of ObMan:VISOR to be 1:2. The model is trained using a batch size of 64 and a learning rate of $1e-5$ across 4 NVIDIA A40 GPUs. We set the loss weights as $\lambda_{\text{visual-hull}} = 1$, $\lambda_{\text{consistency}} = 1$ and $\lambda_{\text{shape-prior}} = 0.25$. Please refer to the supplementary for more details.

5.1. Results

Effectiveness of our supervision cues. We first examine if the indirect supervision from visual hull and shape prior is useful for object generalization. We evaluate on both MOW

Method	Supervision (ObMan +)	F@5 ↑	F@10 ↑	CD ↓
AC-SDF [74]	-	0.17	0.32	3.72
Ours (HORSE)	HO3D (Multi-view 2D)	0.23	0.43	1.41
HO [24]	HO3D (3D)	0.11	0.22	4.19
GF [32]	HO3D (3D)	0.12	0.24	4.96
AC-SDF [74]	HO3D (3D)	0.30	0.53	1.11

Table 2: View generalization on HO3D. We report F-score at 5mm & 10 mm and Chamfer distance (CD, mm) for view generalization on HO3D dataset from [74]. Our approach (even without any 3D supervision) outperforms HO [24] and GF [32], trained on HO3D with full 3D supervision. Our multi-view training method is able to bridge more than 40% of the gap between no training on HO3D to training with full 3D supervision.

	F@5 ↑	F@10 ↑	CD ↓
HORSE (base setting)	0.234	0.434	1.41
no training on HO3D	0.175	0.329	3.72
w/o filtering	0.213	0.405	1.42
w/ ground truth object pose ¹	0.243	0.444	1.39

Table 3: Analysis of supervision quality on HO3D. We assess the quality of 2D mask supervision used in our method. We observe that automated filtering to remove incorrect hand poses (Sec. 4) improves supervision quality & using ground truth hand pose does not cause much difference compared to using predicted hand pose.¹

& HO3D datasets in Tab. 1 and compare with AC-OCC & AC-SDF trained on different combinations of ObMan, HO3D & MOW datasets with 3D supervision. Our approach provides gains of more than 20% across all metrics compared to AC-OCC trained on ObMan. This shows the benefits of our supervision cues over training on just synthetic data. We also outperform AC-SDF trained on HO3D with full 3D supervision & evaluated on MOW, and AC-SDF trained on MOW with full 3D supervision & evaluated on HO3D. This indicates that our indirect supervision cues from in-the-wild VISOR dataset are useful for generalizing to novel objects, both in in-the-wild MOW and HO3D lab settings.

Occupancy vs SDF. We also observe that the SDF formulation performs better than occupancy when trained with full 3D supervision (AC-OCC vs. AC-SDF). This is in contrast to results in our indirect supervision setting where we find the SDF training is unstable and does not give meaningful predictions. This could be because regressing continuous SDF values in a weakly supervised manner is harder than binary classification. We also find that AC-SDF does not consistently benefit from training on real-world datasets with 3D ground truth due to the small size of such datasets, potentially leading to overfitting on small numbers of objects.

View generalization results on HO3D. From the results in Tab. 2, we observe gains with using supervision cues over just training on synthetic data, consistent with trends in the object generalization setting. Moreover, we also outperform

$\mathcal{L}_{\text{ObMan}}$	$\mathcal{L}_{\text{visual-hull}}$	$\mathcal{L}_{\text{consistency}}$	$\mathcal{L}_{\text{shape-prior}}$	F@5 ↑	F@10 ↑	CD ↓
✓				0.095	0.181	8.69
✓	✓			0.111	0.205	7.26
✓		✓		0.073	0.132	12.75
✓	✓	✓		0.117	0.216	6.93
✓	✓	✓	✓	0.121	0.220	6.76

Table 4: Role of different loss functions. We report F-score at 5mm & 10 mm and Chamfer distance (CD, mm) for different variants of our model on MOW. We observe that all losses are effective. Our multiview mask supervision leads to the largest gain.

Dataset	F@5 ↑	F@10 ↑	CD ↓
ObMan	0.095	0.181	8.69
ObMan + VISOR	0.117	0.216	6.93
ObMan + VISOR + HO3D	0.121	0.221	6.71
ObMan + VISOR + HO3D + Core50	0.123	0.223	6.65

Table 5: Scaling up datasets. Since our approach does not require 3D supervision, we can also scale it up by incorporating additional hand-object interaction datasets. Here, we consider 2 extra datasets - HO3D & Core50, and observe gradual improvement on F-score at 5mm & 10 mm and Chamfer distance (CD, mm) metrics.

HO [24] & GF [32], both of which are trained on HO3D using full 3D ground truth as supervision. In fact, our models outperform these methods even when our model doesn’t have access to any images from the HO3D dataset (last row in Tab. 1 vs. GF and HO performance in Table 2). We believe this is because of our use of more expressive pixel-aligned features and hand articulation features. AC-SDF trained on HO3D with full 3D supervision serves as an upper bound on the performance obtainable in this *view generalization setting* with models of comparable capacity.

5.2. Ablation Study

Analysis of supervision quality. We also observe in Tab. 2 that our method is able to bridge more than 40% of the gap between no training on HO3D to training with full 3D supervision. We further use the view generalization setting to assess the quality of 2D object mask supervision used in our method in Tab. 3. Our automated filtering of frames with inaccurate hand poses (as described in Sec. 4) is crucial for good performance. Also, little is lost from using hand pose as a proxy for object pose on the HO3D dataset.¹

Role of different loss terms. We experiment with multiple variants of our model to assess the importance of different loss terms. We start with the AC-OCC model trained on ObMan and gradually add $\mathcal{L}_{\text{visual-hull}}$, $\mathcal{L}_{\text{consistency}}$, and $\mathcal{L}_{\text{shape-prior}}$.

¹While prior work [74] has used similar contrast between performance with predicted hands vs. ground truth hands to make claims, we note that those claims and this result should both be taken with a grain of salt. The publicly available FrankMocap model is trained on HO3D, so its predictions on HO3D are better than they would be on unseen data. As most of our models train on the VISOR dataset (not used for training FrankMocap), the other experiments reported in our work do not suffer from this issue.

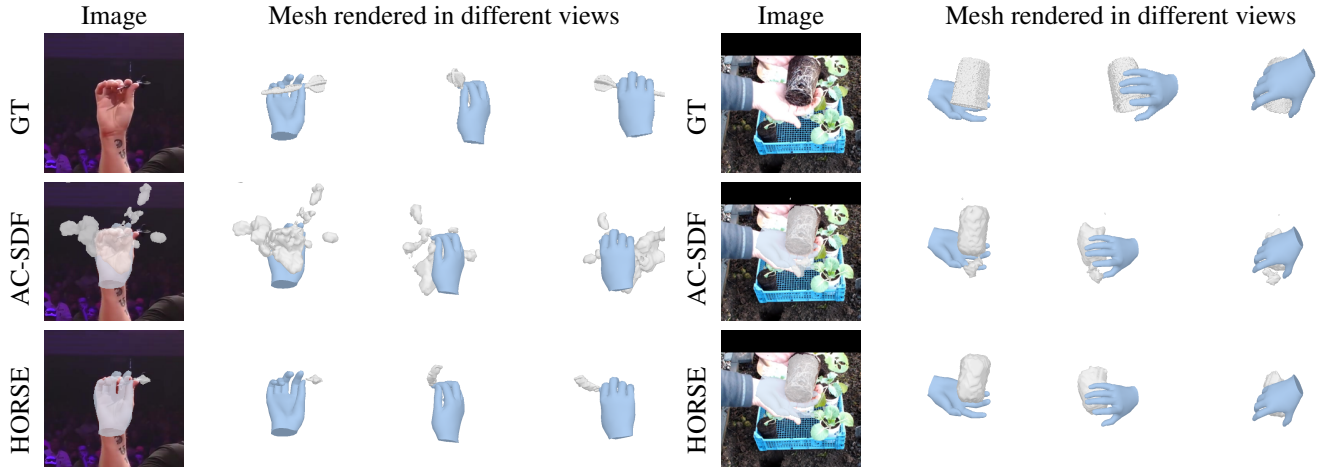


Figure 6: Mesh visualizations on MOW object generalization split. We show the object mesh projected onto the image and rendered in different views for our HORSE model and compare with the AC-SDF model trained on ObMan dataset with 3D supervision (best baseline model). We also show the ground truth (GT) object model. We observe that our model is able to predict the object shape more accurately than AC-SDF which often reconstructs smaller and disconnected shapes.

From the results in Tab. 4, we observe that $\mathcal{L}_{\text{visual-hull}}$ is more effective than $\mathcal{L}_{\text{consistency}}$ and using them together provides further benefits. Moreover, $\mathcal{L}_{\text{shape-prior}}$ improves performance on top of $\mathcal{L}_{\text{consistency}}$ and $\mathcal{L}_{\text{visual-hull}}$.

Scaling up datasets. Since our framework does not require 3D supervision, we can incorporate more video datasets for training. Tab. 5 shows the effect of scaling up the amount of multi-view data used for training our model. We incrementally train on VISOR (approx. 400 unique objects), HO3D (10 unique objects), and Core50 [35] (50 unique objects) datasets in addition to ObMan pretraining and observe gradual improvements. VISOR is by far the most diverse dataset and hence leads to the largest increase in performance.

5.3. Visualizations

We compare the mesh generated by our model and AC-SDF trained on ObMan in Fig. 6. For this, we sample points uniformly in a $64 \times 64 \times 64$ volume, predict their occupancies or SDF from the network and run the marching cubes algorithm. We project the mesh into the input image and render it in different views. We observe that our model is able to capture the visual hull of the object, as evidenced by the projection of the mesh onto the image. Moreover, our model generates more coherent shapes than AC-SDF, which often reconstructs disconnected and scattered shapes. More results and visualizations are provided in supplementary.

5.4. Limitations

Inaccurate hand pose. Our approach is dependent on predictions from FrankMocap for hand pose and camera parameters. We observe that the sampled points do not cover the entire object if the hand pose is not accurate, due to mis-projection into the image plane. This leads to exclusion of

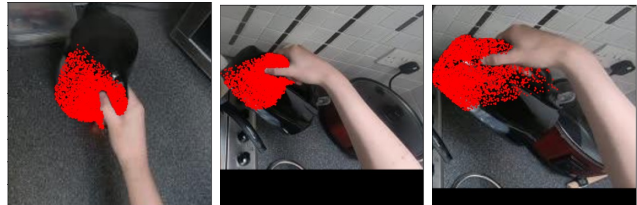


Figure 7: Limitations. Since we rely on FrankMocap predictions for projection into the image, we observe that the **sampled** points do not cover the entire object if the hand pose is not accurate. Also, there are several cases in our incidental multiview setting where the 360° view of the object is not captured, *e.g.* kettle in the figure.

points in certain parts of the object (Fig. 7).

Limited object views. Using in-the-wild data for multiview supervision, we observe several cases where the 360° view of the object is not captured, *e.g.* kettle in Fig. 7. This is in contrast to the datasets collected in lab settings where the subject is often instructed to move the object or a multi-camera capture setup is used to capture all sides of the object.

6. Conclusion

We present an approach for reconstructing hand-held objects in 3D from a single image. We leverage multiview 2D supervision from in-the-wild VISOR [11] videos, and data-driven 3D shape priors from synthetic ObMan dataset to circumvent the need for direct 3D supervision. Our experiments in object generalization setting on MOW and HO3D datasets indicate that our approach generalizes better to novel objects than baselines trained using 3D supervision. Future directions include jointly optimizing the hand pose with the object shape at training time to deal with inaccurate hand pose from FrankMocap. Furthermore, additional cues, *e.g.* contact priors from large-scale datasets can also be useful.

Acknowledgements: We thank Ashish Kumar, Erin Zhang, Arjun Gupta, Shaowei Liu, Anand Bhattad and Pranay Thangeda for feedback on the draft. This material is based upon work supported by NSF (IIS2007035), NASA (80NSSC21K1030), DARPA (Machine Common Sense program), an Amazon Research Award, an NVIDIA Academic Hardware Grant, and the NCSA Delta System (supported by NSF OCI 2005572 and the State of Illinois).

References

- [1] Sameer Agarwal, Noah Snavely, Ian Simon, Steven M. Seitz, and Richard Szeliski. Building rome in a day. In *Proceedings of the IEEE International Conference on Computer Vision (ICCV)*, 2009. 3
- [2] John Aliomonos and Michael J. Swain. Shape from texture. In *Proceedings of the International Joint Conference on Artificial Intelligence (IJCAI)*, 1985. 3
- [3] Yuval Bahat and Gregory Shakhnarovich. Confidence from invariance to image transformations. *arXiv*, 2018. 5
- [4] Christian Bailer, Manuel Finckh, and Hendrik Lensch. Scale robust multi view stereo. In *Proceedings of the European Conference on Computer Vision (ECCV)*, 2012. 3
- [5] Gavin Buckingham. Hand tracking for immersive virtual reality: Opportunities and challenges. *Frontiers in Virtual Reality*, 2021. 1
- [6] Alan Bundy and Lincoln Wallen. *Shape from Texture*, pages 122–122. Springer Berlin Heidelberg, 1984. 3
- [7] Zhe Cao, Ilija Radosavovic, Angjoo Kanazawa, and Jitendra Malik. Reconstructing hand-object interactions in the wild. In *Proceedings of the IEEE International Conference on Computer Vision (ICCV)*, 2021. 2, 3, 4, 5, 6
- [8] Angel X. Chang, Thomas A. Funkhouser, Leonidas J. Guibas, Pat Hanrahan, Qixing Huang, Zimo Li, Silvio Savarese, Manolis Savva, Shuran Song, Hao Su, Jianxiong Xiao, L. Yi, and Fisher Yu. Shapenet: An information-rich 3D model repository. *ArXiv*, 2015. 3, 4
- [9] Dima Damen, Hazel Doughty, Giovanni Maria Farinella, Sanja Fidler, Antonino Furnari, Evangelos Kazakos, Davide Moltisanti, Jonathan Munro, Toby Perrett, Will Price, and Michael Wray. Scaling egocentric vision: The epic-kitchens dataset. *Proceedings of the European Conference on Computer Vision (ECCV)*, 2018. 2
- [10] Dima Damen, Hazel Doughty, Giovanni Maria Farinella, Sanja Fidler, Antonino Furnari, Evangelos Kazakos, Davide Moltisanti, Jonathan Munro, Toby Perrett, Will Price, and Michael Wray. The epic-kitchens dataset: Collection, challenges and baselines. *IEEE Transactions on Pattern Analysis and Machine Intelligence (TPAMI)*, 2020. 5
- [11] Ahmad Darkhalil, Dandan Shan, Bin Zhu, Jian Ma, Amlan Kar, Richard Higgins, Sanja Fidler, David Fouhey, and Dima Damen. Epic-kitchens visor benchmark: Video segmentations and object relations. In *NeurIPS Track on Datasets and Benchmarks*, 2022. 2, 3, 4, 5, 8
- [12] Patrick Etyngier, Florent Ségonne, and Renaud Keriven. Shape priors using manifold learning techniques. In *Proceedings of the IEEE International Conference on Computer Vision (ICCV)*, 2007. 3
- [13] Keith Forbes, Fred Nicolls, Gerhard de Jager, and Anthon Voigt. Shape-from-silhouette with two mirrors and an uncalibrated camera. In *Proceedings of the European Conference on Computer Vision (ECCV)*, 2006. 3
- [14] Jan-Michael Frahm, Pierre Fite-Georgel, David Gallup, Tim Johnson, Rahul Raguram, Changchang Wu, Yi-Hung Jen, Enrique Dunn, Brian Clipp, Svetlana Lazebnik, and Marc Pollefeys. Building rome on a cloudless day. In *Proceedings of the European Conference on Computer Vision (ECCV)*, 2010. 3
- [15] Yasutaka Furukawa, Brian Curless, Steven M. Seitz, and Richard Szeliski. Towards internet-scale multi-view stereo. In *Proceedings of the IEEE Conference on Computer Vision and Pattern Recognition (CVPR)*, 2010. 3
- [16] Yasutaka Furukawa and Jean Ponce. Accurate, dense, and robust multi-view stereopsis. *IEEE Transactions on Pattern Analysis and Machine Intelligence (TPAMI)*, 2010. 3
- [17] Silvano Galliani, Katrin Lasinger, and Konrad Schindler. Massively parallel multiview stereopsis by surface normal diffusion. In *ICCV*, 2015. 3
- [18] Ian Goodfellow, Jean Pouget-Abadie, Mehdi Mirza, Bing Xu, David Warde-Farley, Sherjil Ozair, Aaron Courville, and Yoshua Bengio. Generative adversarial nets. In *Advances in Neural Information Processing Systems (NeurIPS)*, 2014. 2, 4
- [19] Kristen Grauman, Andrew Westbury, Eugene Byrne, Zachary Chavis, Antonino Furnari, Rohit Girdhar, Jackson Hamburger, Hao Jiang, Miao Liu, Xingyu Liu, et al. Ego4d: Around the world in 3,000 hours of egocentric video. In *Proceedings of the IEEE Conference on Computer Vision and Pattern Recognition (CVPR)*, 2022. 2
- [20] Shreyas Hampali, Mahdi Rad, Markus Oberweger, and Vincent Lepetit. Honnotate: A method for 3d annotation of hand and object poses. In *Proceedings of the IEEE Conference on Computer Vision and Pattern Recognition (CVPR)*, 2020. 4
- [21] Shangchen Han, Beibei Liu, Randi Cabezas, Christopher D. Twigg, Peizhao Zhang, Jeff Petkau, Tsz-Ho Yu, Chun-Jung Tai, Muzaffer Akbay, Zheng Wang, Asaf Nitzan, Gang Dong, Yuting Ye, Lingling Tao, Chengde Wan, and Robert Wang. Megatrack: monochrome egocentric articulated hand-tracking for virtual reality. *ACM Transactions on Graphics (TOG)*, 2020. 1
- [22] Richard Hartley and Andrew Zisserman. *Multiple view geometry in computer vision*. Cambridge university press, 2003. 2, 3
- [23] Yana Hasson, Bugra Tekin, Federica Bogo, Ivan Laptev, Marc Pollefeys, and Cordelia Schmid. Leveraging photometric consistency over time for sparsely supervised hand-object reconstruction. *Proceedings of the IEEE Conference on Computer Vision and Pattern Recognition (CVPR)*, 2020. 3
- [24] Yana Hasson, Gül Varol, Dimitris Tzionas, Igor Kalevatykh, Michael J. Black, Ivan Laptev, and Cordelia Schmid. Learning joint reconstruction of hands and manipulated objects. In *Proceedings of the IEEE Conference on Computer Vision and Pattern Recognition (CVPR)*, 2019. 2, 3, 4, 5, 6, 7
- [25] Kaiming He, Georgia Gkioxari, Piotr Dollár, and Ross B. Girshick. Mask R-CNN. In *Proceedings of the IEEE In-*

- ternational Conference on Computer Vision (ICCV), 2017. 4
- [26] Kaiming He, X. Zhang, Shaoqing Ren, and Jian Sun. Deep residual learning for image recognition. *Proceedings of the IEEE Conference on Computer Vision and Pattern Recognition (CVPR)*, 2016. 4
- [27] Jared Heinly, Johannes Lutz Schönberger, Enrique Dunn, and Jan-Michael Frahm. Reconstructing the World* in Six Days *(As Captured by the Yahoo 100 Million Image Dataset). In *Proceedings of the IEEE Conference on Computer Vision and Pattern Recognition (CVPR)*, 2015. 3
- [28] Di Huang, Xiaopeng Ji, Xingyi He, Jiaming Sun, Tong He, Qing Shuai, Wanli Ouyang, and Xiaowei Zhou. Reconstructing hand-held objects from monocular video. In *ACM Transactions on Graphics*, 2022. 3
- [29] Hanwen Jiang, Shaowei Liu, Jiashun Wang, and Xiaolong Wang. Hand-object contact consistency reasoning for human grasps generation. In *Proceedings of the IEEE International Conference on Computer Vision (ICCV)*, 2021. 2
- [30] Angjoo Kanazawa, Shubham Tulsiani, Alexei A Efros, and Jitendra Malik. Learning category-specific mesh reconstruction from image collections. In *Proceedings of the European Conference on Computer Vision (ECCV)*, 2018. 3, 5
- [31] Abhishek Kar, Shubham Tulsiani, Joao Carreira, and Jitendra Malik. Category-specific object reconstruction from a single image. In *Proceedings of the IEEE Conference on Computer Vision and Pattern Recognition (CVPR)*, 2015. 3
- [32] Korrawe Karunratanakul, Jinlong Yang, Yan Zhang, Michael J Black, Krikamol Muandet, and Siyu Tang. Grasping field: Learning implicit representations for human grasps. In *Proceedings of the International Conference on 3D Vision (3DV)*, 2020. 2, 3, 6, 7
- [33] Nilesh Kulkarni, Abhinav Gupta, David F. Fouhey, and Shubham Tulsiani. Articulation-aware canonical surface mapping. In *Proceedings of the IEEE Conference on Computer Vision and Pattern Recognition (CVPR)*, 2020. 3
- [34] Aldo Laurentini. The visual hull concept for silhouette-based image understanding. *IEEE Transactions on Pattern Analysis and Machine Intelligence (TPAMI)*, 16:150–162, 1994. 4
- [35] Vincenzo Lomonaco and Davide Maltoni. Core50: a new dataset and benchmark for continuous object recognition. In *Proceedings of the Conference on Robot Learning (CoRL)*, 2017. 8
- [36] Wei-Chiu Ma, Anqi Joyce Yang, Shenlong Wang, Raquel Urtasun, and Antonio Torralba. Virtual correspondence: Humans as a cue for extreme-view geometry. In *Proceedings of the IEEE Conference on Computer Vision and Pattern Recognition (CVPR)*, 2022. 3
- [37] Priyanka Mandikal and Kristen Grauman. Dexvip: Learning dexterous grasping with human hand pose priors from video. In *Proceedings of the Conference on Robot Learning (CoRL)*, 2021. 1
- [38] Priyanka Mandikal and Kristen Grauman. Learning dexterous grasping with object-centric visual affordances. In *Proceedings of the IEEE International Conference on Robotics and Automation (ICRA)*, 2021. 1
- [39] Xudong Mao, Qing Li, Haoran Xie, Raymond Y. K. Lau, Zhen Wang, and Stephen Paul Smolley. Least squares generative adversarial networks. In *Proceedings of the IEEE International Conference on Computer Vision (ICCV)*, 2017. 5
- [40] Daniel Maturana and Sebastian A. Scherer. Voxnet: A 3d convolutional neural network for real-time object recognition. In *Proceedings of the International Conference on Intelligent Robots and Systems (IROS)*, 2015. 3
- [41] Wojciech Matusik, Chris Buehler, Ramesh Raskar, Steven J Gortler, and Leonard McMillan. Image-based visual hulls. In *ACM Transactions on Graphics*, 2000. 4
- [42] Lars Mescheder, Michael Oechsle, Michael Niemeyer, Sebastian Nowozin, and Andreas Geiger. Occupancy networks: Learning 3d reconstruction in function space. In *Proceedings of the IEEE Conference on Computer Vision and Pattern Recognition (CVPR)*, 2019. 2, 3, 6
- [43] Ben Mildenhall, Pratul P. Srinivasan, Matthew Tancik, Jonathan T. Barron, Ravi Ramamoorthi, and Ren Ng. Nerf: Representing scenes as neural radiance fields for view synthesis. In *Proceedings of the European Conference on Computer Vision (ECCV)*, 2020. 3
- [44] Andrew T Miller and Peter K Allen. Graspit! a versatile simulator for robotic grasping. *IEEE Robotics & Automation Magazine*, 2004. 6
- [45] Michael Niemeyer, Lars M. Mescheder, Michael Oechsle, and Andreas Geiger. Differentiable volumetric rendering: Learning implicit 3d representations without 3d supervision. In *Proceedings of the IEEE Conference on Computer Vision and Pattern Recognition (CVPR)*, 2020. 2, 6
- [46] Jeong Joon Park, Peter Florence, Julian Straub, Richard Newcombe, and Steven Lovegrove. DeepSDF: Learning continuous signed distance functions for shape representation. In *Proceedings of the IEEE Conference on Computer Vision and Pattern Recognition (CVPR)*, 2019. 2, 3, 6
- [47] Charles Ruizhongtai Qi, Hao Su, Kaichun Mo, and Leonidas J. Guibas. Pointnet: Deep learning on point sets for 3d classification and segmentation. In *Proceedings of the IEEE Conference on Computer Vision and Pattern Recognition (CVPR)*, 2017. 3
- [48] Charles Ruizhongtai Qi, Li Yi, Hao Su, and Leonidas J. Guibas. Pointnet++: Deep hierarchical feature learning on point sets in a metric space. In *Advances in Neural Information Processing Systems (NeurIPS)*, 2017. 3
- [49] Yuzhe Qin, Hao Su, and Xiaolong Wang. From one hand to multiple hands: Imitation learning for dexterous manipulation from single-camera teleoperation. *Proceedings of the International Conference on Intelligent Robots and Systems (IROS)*, 2022. 1
- [50] Yuzhe Qin, Yueh-Hua Wu, Shaowei Liu, Hanwen Jiang, Ruihan Yang, Yang Fu, and Xiaolong Wang. Dexmv: Imitation learning for dexterous manipulation from human videos. In *Proceedings of the European Conference on Computer Vision (ECCV)*, 2022. 1
- [51] Hans Rijkema and Michael Girard. Computer animation of knowledge-based human grasping. In James J. Thomas, editor, *ACM Transactions on Graphics*, 1991. 2

- [52] Chris Rockwell and David F Fouhey. Full-body awareness from partial observations. In *Proceedings of the European Conference on Computer Vision (ECCV)*, 2020. 5
- [53] Grégory Rogez, Maryam Khademi, JS Supančič III, Jose Maria Martinez Montiel, and Deva Ramanan. 3d hand pose detection in egocentric rgb-d images. In *Proceedings of the European Conference on Computer Vision (ECCV)*, 2014. 3
- [54] Javier Romero, Hedvig Kjellström, and Danica Kragic. Hands in action: real-time 3D reconstruction of hands in interaction with objects. In *Proceedings of the IEEE International Conference on Robotics and Automation (ICRA)*, 2010. 2, 3
- [55] Javier Romero, Dimitrios Tzionas, and Michael J Black. Embodied hands: Modeling and capturing hands and bodies together. *ACM Transactions on Graphics (ToG)*, 2017. 3
- [56] Yu Rong, Takaaki Shiratori, and Hanbyul Joo. Frankmocap: Fast monocular 3D hand and body motion capture by regression and integration. *Proceedings of the IEEE International Conference on Computer Vision Workshops (ICCV Workshops)*, 2021. 1, 2, 3, 5
- [57] Shunsuke Saito, Zeng Huang, Ryota Natsume, Shigeo Morishima, Angjoo Kanazawa, and Hao Li. Pifu: Pixel-aligned implicit function for high-resolution clothed human digitization. *Proceedings of the IEEE International Conference on Computer Vision (ICCV)*, 2019. 4
- [58] F. Schaffalitzky and A. Zisserman. Multi-view matching for unordered image sets, or “how do i organize my holiday snaps?”. In *Proceedings of the European Conference on Computer Vision (ECCV)*, 2002. 3
- [59] Johannes Lutz Schönberger and Jan-Michael Frahm. Structure-from-motion revisited. In *Proceedings of the IEEE Conference on Computer Vision and Pattern Recognition (CVPR)*, 2016. 1, 2, 3, 6
- [60] Johannes Lutz Schönberger, Enliang Zheng, Marc Pollefeys, and Jan-Michael Frahm. Pixelwise view selection for unstructured multi-view stereo. In *Proceedings of the European Conference on Computer Vision (ECCV)*, 2016. 2, 3, 6
- [61] Johannes L. Schönberger, Filip Radenović, Ondrej Chum, and Jan-Michael Frahm. From single image query to detailed 3d reconstruction. In *Proceedings of the IEEE Conference on Computer Vision and Pattern Recognition (CVPR)*, 2015. 3
- [62] Dandan Shan, Jiaqi Geng, Michelle Shu, and David F Fouhey. Understanding human hands in contact at internet scale. In *Proceedings of the IEEE Conference on Computer Vision and Pattern Recognition (CVPR)*, 2020. 2, 3
- [63] Qi Shan, Riley Adams, Brian Curless, Yasutaka Furukawa, and Steven Seitz. The visual turing test for scene reconstruction. In *Proceedings of the International Conference on 3D Vision (3DV)*, 2013. 3
- [64] Qi Shan, Brian Curless, Yasutaka Furukawa, Carlos Hernandez, and Steven M. Seitz. Occluding contours for multi-view stereo. In *Proceedings of the IEEE Conference on Computer Vision and Pattern Recognition (CVPR)*, 2014. 3
- [65] Noah Snavely, Steven M. Seitz, and Richard Szeliski. Photo tourism: Exploring photo collections in 3d. *ACM Transactions on Graphics (ToG)*, 2006. 3
- [66] Maxim Tatarchenko, Stephan R Richter, René Ranftl, Zhuwen Li, Vladlen Koltun, and Thomas Brox. What do single-view 3d reconstruction networks learn? In *Proceedings of the IEEE Conference on Computer Vision and Pattern Recognition (CVPR)*, 2019. 6
- [67] Mukhiddin Toshpulatov, Wookey Lee, Suan Lee, and Arousha Haghighian Roudsari. Human pose, hand and mesh estimation using deep learning: a survey. *The Journal of Supercomputing*, 2022. 3
- [68] Shubham Tulsiani, Alexei A. Efros, and Jitendra Malik. Multi-view consistency as supervisory signal for learning shape and pose prediction. In *Proceedings of the IEEE Conference on Computer Vision and Pattern Recognition (CVPR)*, 2018. 3
- [69] Dylan Turpin, Liquan Wang, Eric Heiden, Yun-Chun Chen, Miles Macklin, Stavros Tsogkas, Sven J. Dickinson, and Animesh Garg. Grasp’d: Differentiable contact-rich grasp synthesis for multi-fingered hands. In *Proceedings of the European Conference on Computer Vision (ECCV)*, 2022. 2
- [70] Dimitrios Tzionas and Juergen Gall. 3d object reconstruction from hand-object interactions. In *Proceedings of the IEEE International Conference on Computer Vision (ICCV)*, 2015. 3
- [71] Yueh-Hua Wu, Jiashun Wang, and Xiaolong Wang. Learning generalizable dexterous manipulation from human grasp affordance. In *Proceedings of the Conference on Robot Learning (CoRL)*, 2022. 1
- [72] Lior Yariv, Yoni Kasten, Dror Moran, Meirav Galun, Matan Atzmon, Ronen Basri, and Yaron Lipman. Multiview neural surface reconstruction by disentangling geometry and appearance. In *Advances in Neural Information Processing Systems (NeurIPS)*, 2020. 2, 6
- [73] Jianglong Ye, Jiashun Wang, Binghao Huang, Yuzhe Qin, and Xiaolong Wang. Learning continuous grasping function with a dexterous hand from human demonstrations. *arXiv*, 2022. 1
- [74] Yufei Ye, Abhinav Gupta, and Shubham Tulsiani. What’s in your hands? 3D reconstruction of generic objects in hands. In *Proceedings of the IEEE Conference on Computer Vision and Pattern Recognition (CVPR)*, 2022. 2, 3, 5, 6, 7
- [75] Yufei Ye, Shubham Tulsiani, and Abhinav Gupta. Shelf-supervised mesh prediction in the wild. In *Proceedings of the IEEE Conference on Computer Vision and Pattern Recognition (CVPR)*, 2021. 3
- [76] Ruo Zhang, Ping-Sing Tsai, James Edwin Cryer, and Mubarak Shah. Shape from shading: A survey. *IEEE Transactions on Pattern Analysis and Machine Intelligence (TPAMI)*, 1999. 3
- [77] Enliang Zheng, Enrique Dunn, Vladimir Jojic, and Jan-Michael Frahm. Patchmatch based joint view selection and depthmap estimation. In *Proceedings of the IEEE Conference on Computer Vision and Pattern Recognition (CVPR)*, 2014. 3
- [78] Enliang Zheng and Changchang Wu. Structure from motion using structure-less resection. In *Proceedings of the IEEE International Conference on Computer Vision (ICCV)*, 2015. 3
- [79] Tinghui Zhou, Matthew Brown, Noah Snavely, and David G Lowe. Unsupervised learning of depth and ego-motion from video. In *Proceedings of the IEEE Conference on Computer Vision and Pattern Recognition (CVPR)*, 2017. 3
- [80] Christian Zimmermann and Thomas Brox. Learning to estimate 3d hand pose from single rgb images. In *Proceedings*

of the IEEE International Conference on Computer Vision (ICCV), 2017. 3

- [81] Berk Çalli, Arjun Singh, Aaron Walsman, Siddhartha S. Srinivasa, P. Abbeel, and Aaron M. Dollar. The ycb object and model set: Towards common benchmarks for manipulation research. In *Proceedings of the International Conference on Advanced Robotics (ICAR)*, 2015. 5